Research Square

Preprints are preliminary reports that have not undergone peer review.
They should not be considered conclusive, used to inform clinical practice,
or referenced by the media as validated information.

Enhancing DC Resistivity Data Two-Dimensional Inversion Result by Using U-Net Based Deep Learning- Algorithm: Examples from Archaegeophysical Surveys

Demet ÖVER
Ankara University
M. Emin CANDANSAYAR
candansayar@ankara.edu.tr
Ankara University

Research Article

Keywords: DCR, Inversion, Deep Learning, 2D, archaeogeophysics

Posted Date: January 2nd, 2024

DOI: https://doi.org/10.21203/rs.3.rs-3796819/v1

License: This work is licensed under a Creative Commons Attribution 4.0 International License.
Read Full License

Additional Declarations: No competing interests reported.

Version of Record: A version of this preprint was published at Journal of Applied Geophysics on June 1st, 2024. See the published version at https://doi.org/10.1016/j.jappgeo.2024.105430.

Abstract

In this study, we suggested using a convolutional neural network (CNN) based algorithm to enhance two-dimensional (2D) Direct Current Resistivity data inversion results. We developed U-net based CNN algorithm, named DCR_Net_Archeo. We generated 1080 sets of 2D resistivity models that simulate buried archeological remains. We calculated synthetic data for those models for different electrode arrays. We added 2% random noise to apparent resistivity data sets and inverted those data sets. We used the 2D inversion results as input and the corresponding real resistivity model as output. By using those 1080 input and output data sets we developed the DCR_Net_Archeo algorithm. First, we tested this algorithm by using synthetic data. We showed that the developed algorithm improved the 2D classical smoothing regularization inversion and the buried body's location and depth can be found very close to the real model. Afterward, we also tested the developed algorithm with real data collected from two different archaeological sites. We showed that the buried wall cross-section location and depth are better found by the DCR_Net_Archeo algorithm than the classical inversion result if we compare it with the excavated wall structure.

1. Introduction

The Direct Current Resistivity (DCR) method is one of the oldest applied geophysical methods. It has been used for various applied geophysical applications such as hydrogeophysical investigations (e.g. Binley and Kemna 2005; Soupios et al. 2007; Demirci et al. 2020), mining geophysics (e.g. Parasnis, 2013; Özyildirim et al. 2020), site investigation (e.g. Chambers et al. 2006; Wisen et al. 2008; Gündoğdu et al. 2020), archeogeophysics studies (Papadopoulos et al. 2006; Candansayar 2008; Gündoğdu et al. 2017).

Generally, DCR data have been collected along a line of sounding-profiling data with multi-channel and multi-electrode data acquisition systems for the last three decades. The sounding-profiling data sets are interpreted by using a two-dimensional (2D) inversion algorithm (e.g., Candansayar 2008; Loke et al. 2018). Combined DCR data sets collected along parallel lines are also inverted by using three-dimensional (3D) inversion algorithms (e.g. Günther et al. 2006; Gündoğdu et al. 2018).

DCR data inverse problem is non-linear and ill-conditioned. Therefore, in general, the Tikhonov regularization method with smoothing stabilizers is used in 2D and 3D DCR data inversion algorithms (Sasaki 1989, 1994; Candansayar, 2008; Loke et al. 2018). In general, we do not have a priori resistivity information of the survey area so a homogenous initial model is used in 2D and 3D DCR data inversion. The average of apparent resistivity data is used as homogenous medium resistivity. Henceforth, we obtain the smooth inversion result. We do not know the underground resistivity structure and the smooth inversion result allows us to roughly interpret the underground resistivity structure.

To obtain more focused inversion results, the researcher suggested using different stabilizing functional instead of smoothing stabilizing functional for 2D and 3D DCR data inversion (Blaschek et al. 2008; Gündoğdu and Candansayar 2018; Gündoğdu et al. 2020; Thibaut 2021; Song et al. 2022). In those

studies, regularized inversion with minimum support and minimum gradient support stabilizer gives a sharper boundary than regularized inversion with smoothing stabilizer. On the other hand, to combine different geophysical methods advantage and obtain sharper 2D inversion results, joint 2D inversion of those data sets are suggested (e.g. Sasaki 1989; Gallardo and Meju 2003; Candansayar and Tezkan 2008; Demirci et al.2017; Özyıldırım et al. 2020).

Inversion with different stabilizing functional or joint inversion of DCR data with other geophysical data such as Radiomagnetotelluric and seismic are improving the inverted resistivity model and resistivity boundaries are resolved in more detail. However, if we investigate sharp boundary structures such as buried archaeological remains, the above-mentioned approaches still find some smooth models. In reality, the resolution decreases with increasing depth in the DCR method such as all the other geophysical methods. Lateral resolution is also depending on the consecutive electrode spacing and size of the anomalous body. Therefore, regularized smoothing inversion of DCR data can be acceptable for most of the applications. However, sharp boundaries of the buried archaeological structures cannot resolve well with a 2D regularized inversion solution.

Artificial neural network (ANN) algorithms have also been used for 2D DCR data imaging in the last two decades (Neyamadpour et al. 2009; Aleardi et al. 2021). In last couple of years, Convolutional Neural Network (CNN) based U-Net architecture (Liu et al. 2020, 2023a; Zhang et al. 2021; Guo et al. 2023; Hiskiawan et al., 2023) and SegNet architecture (Vu and Jardani 2021; Wilson et al. 2022; Jia et al. 2022) has been alternative to ANN algorithm for 2D/3D resistivity imaging. In most of the above-mentioned ANN and CNN-based algorithms, observed data (apparent resistivity) sets are used as input, and 2D resistivity models are used as output (Liu et al. 2020; Aleardi et al. 2021; Vu and Jardani 2021; Jia et al. 2022; Wilson et al. 2022). However, apparent resistivity data sets for different electrode arrays can be very different from each other for the same resistivity model. Therefore, the previously developed CNN algorithm for the DCR method such as ERSInvNet (Liu et al. 2020) cannot used for different data sets that are collected for different electrode arrays along the same line. On the other hand, if one compares the 2D inversion results of the data sets collected along the same line for different electrode arrays (such as Wenner-Schlumberger, Dipole-dipole), the inverted resistivity models will be very close to each other. Additionally, it shows data combined 2D inversion of DD, PDL, and PDR arrays data sets give more accurate inversion results than any individual arrays data sets such as Wenner-Schlumberger (WS), Dipole-Dipole (DD), left side Pole-Dipole (PDL) and right-side Pole Dipole (PDR) (Candansayar 2008).

Although alternative usage of stabilizing functionals gives sharper inversion results than the smoothing stabilizer, it still cannot find the bottom boundary of resistive/ (or conductive) structure. In reality, the resolution decreases with increasing depth in the DCR method such as all the other geophysical methods. Lateral resolution is also depending on the consecutive electrode spacing and size of the anomalous body.

To sum up, as mentioned above, if we are investigating some geological structure, a smooth inversion result can be acceptable. However, if we investigate some buried structure that has sharp boundary

structures such as archaeological remains, we need sharper inversion results. CNN-based deep learning algorithm can be one alternative to get a sharp resistivity image. However, as we mentioned above, the previous CNN-based algorithm for 2D DCR data interpretation uses apparent resistivity as input and a real 2D resistivity model as output. This approach can generate some artificial anomaly if one uses a different array of apparent resistivity data collected along the same line. There is just one recent study that suggests using inversion result as input and corresponding real resistivity model as output to develop CNN based algorithm for 2D DCR imaging (Liu et al.2023). They just used 200 sets of inverted 2D resistivity models as input and corresponding 200 sets of real resistivity models as output for developing the CNN-based U-net algorithm. However, in this study, they did not consider the noise effect of the data and the vertical and horizontal resolution of the used electrode array (Wenner). They also did not consider the depth of penetration of the recovered model. Their real data application result also does not represent the full part of the model. Their field data was collected along the 35-meter-length line. However, their inversion result and CNN-based result are given a 32-meter-length line (0.0534x600).

Deep learning algorithms such as CNN-based U-Net architecture were developed for image recognition and reconstruction in different areas such as medical imaging (Aghabiglou and Eksioglu, 2021). In this study, we suggest improving 2D regularized inversion results to get sharper 2D resistivity images by using CNN-based U-Net architecture. In this study, we developed a new deep-learning algorithm that called DCR_NET_ARCHAEO. This algorithm was developed by using 1080 pairs of input and output 2D resistivity models. It is specifically designed for archaeogeophysical surveys to get more sharper resistivity image to reveal buried archaeological remains. In the following sections, we briefly introduce regularized 2D modeling and inversion in the DCR method. Afterward, we explain the developed deep learning algorithm. Finally, we show how the developed DCR2D_Net_Archeo algorithm improves 2D inversion results by using synthetic data calculated for the models that simulate the buried archaeological remains. We also showed the advantage of the developed deep learning algorithm by using two field data collected from two different archaeological sites in Ankara and Kayseri cities from Türkiye.

2. Methods

2.1. 2D Modeling And Inversion

In this study, we used freely available DCR2D modeling and inversion algorithms to generate synthetic data and to invert synthetic and field data (Candansayar 2008). The Poisson equation is solved by using the finite difference technique in the modeling part of this algorithm. In the inversion part of the algorithm, the regularized smoothing inversion method is used. In this approach, the following model correction vector ($\Delta \mathbf{m}$) is solved in each iteration.

$$\left(\mathbf{A}^{\mathbf{T}}\mathbf{W}_{\mathbf{d}}^{\mathbf{T}}\mathbf{W}_{\mathbf{d}}\mathbf{A}+\alpha\mathbf{C}^{\mathbf{T}}\mathbf{C}\right)\Delta\mathbf{m}=\mathbf{A}^{\mathbf{T}}\mathbf{W}_{\mathbf{d}}^{\mathbf{T}}\mathbf{W}_{\mathbf{d}}\mathbf{A}\Delta\mathbf{d}$$

1

where $\mathbf{A}$ is the Jacobian matrix, $\Delta\mathbf{d}$ is the vector of differences between the calculated data and the observed data, m is the parameter correction vector, $\mathbf{C}$ is a Laplacian operator, $\mathbf{W_d}$ is the data weighting matrix and α is a regularization parameter. For more details about the algorithm please refer to Candansayar (2008).

This algorithm is modified to create different resistivity models that simulate buried archaeological remains. Candansayar (2008) showed that combined inversion of left and right side pole-dipole (PDL and PDR) and dipole-dipole (DD) arrays data sets give better resolution than the individual inversion of classical electrode arrays (Wenner, Schlumberger, PDL, PDL, DD) even for the blocks below the beginning and at the end of the electrodes. Therefore, we calculated the synthetic data for PDL and PDR arrays for n = 1,2, …8 levels. Number of data for PDL and PDR arrays is 248. These data sets were calculated for 21 electrodes with 2.5 m consecutive electrode spacing. We divided two blocks between each electrode in the model mesh. The model mesh was created considering the depth of investigation (Oldenburg and Li, 1999) for electrode setup. The inverted resistivity model has 40 and 16 blocks in the x- and z direction, respectively. Note that, during the forward solution we added 8 blocks on the left and right sides and the bottom part of the mesh.

In this study, we created 1080 sets of 2D resistivity model that simulates buried archeological remains. We calculated synthetic data for the created 2D resistivity models and added %2 random noise to each data set. Afterward, we inverted those noise-added data sets individually. In the end, we obtained 1080 inversion results and corresponding real resistivity models. We used 2D inversion results as input and the corresponding 2D resistivity model as output to create a deep learning algorithm in the following section. The real model and inverted model dimensions are (16, 40).

Each inversion process terminated when the normalized root mean square (RMS) error was not improved or it reached 1. If N is the number of data points, RMS is calculated by using the following formula

$$RMS = \sqrt{\frac{(\mathbf{W_d}\Delta\mathbf{d})(\mathbf{W_d}\Delta\mathbf{d})^T}{N}}$$

2

.

2.2. Deep Learning

Deep learning, particularly through neural networks, has shown the ability to recognize patterns. This capability is instrumental in automating the extraction of buried archeological features from 2D DCR inversion results (2D resistivity model). Our research focuses on enhancing traditional DCR inversion results. We achieve this through the integration of Convolutional Neural Networks (CNN). This network is inspired by the renowned U-Net architecture (Fig. 1). We have developed the architecture detailed in this paper using the PyTorch framework.

The U-Net architecture initially conceptualized for semantic segmentation tasks, is characterized by its unique encoder-decoder structure (Ronneberger et al. 2015). This model has been recognized for its effectiveness in various image-processing applications.

At its core, the encoder part of the U-Net model operates by progressively condensing the input image's feature size. This is achieved through a combination of convolutional layers and pooling layers. In these convolutional layers, the network begins by capturing basic, low-level features from the input. As the data progresses deeper into the network, subsequent layers focus on extracting complex, higher-level features. Following the convolutional stages, the network employs down-sampling, commonly through max-pooling layers. This step is crucial as it reduces the size of the feature map, allowing the model to generate a generalized representation of the input data.

The decoder segment of the U-Net architecture functions to expand the condensed feature map from the encoder. It performs this while conducting segmentation on the input image. A key aspect of the decoder is its utilization of information from the encoder. Before each convolutional layer in the decoder, it retrieves feature map data from the corresponding encoder layer. This retrieval is crucial for reconstructing detailed features in the image. This reconstruction process involves the use of transposed convolutional layers or similar operations. Additionally, skip connections are a defining feature of the U-Net architecture. They play a role in transferring feature map sizes from the encoder to the decoder. These connections are essential as they combine both low-level and high-level features from different layers. This combination boosts the network's ability to perform accurate segmentation.

We adjust critical parameters to set the model's learning process for CNN (Table 1). We set the learning rate at 0.001. It strikes a balance between rapid convergence and maintaining stability during training. The incorporation of the ReLU activation function introduces necessary non-linearity into the convolutional neural network processes (Feng and Lu, 2019). Furthermore, batch normalization is implemented in each convolutional layer except the last layer. At the last layer, we used the Sigmoid function (Feng and Lu, 2019). It ensures consistent and reliable gradient behavior, which in turn leads to quicker and more efficient training. A batch size of 32 was chosen to optimize computational resources. Additionally, the Adam optimization algorithm (Hassan et al., 2023) is employed to facilitate effective adjustments in the model's weights during the training process. The training of the network is conducted for 200 epochs, with an early stopping mechanism based on validation performance. This approach helps in achieving convergence while avoiding overfitting.

Training the network involves using synthetic models to ensure the model learns a wide range of features and patterns. After the training phase, the network undergoes testing. This testing phase includes both additional sets of synthetic data and field data. Such a comprehensive testing approach is crucial to validate the network's applicability and performance across various scenarios.

2.2.1. Development of DCR2D_Net_Archeo algorithm

In this study, we introduce a deep learning algorithm, DCR2D_Net_Archeo, based on the above-mentioned U-Net architecture. To construct the DCR2D_Net_Archeo algorithm, we used a 1080 real and inverted resistivity model. The real and inverted resistivity models are generated in 174 minutes (2.9 Hours) of CPU time by using with DCR2D algorithm. We allocated 900 data sets for training, 84 data sets for testing, and 96 for validation. The DCR2D_Net_Archeo algorithm was generated in 78 minutes by using the PyTorch library on the Phyton platform. We used a Desktop PC that has 48GB RAM and an Intel(R) Core(TM) i7-5930K CPU to create a 1080 data set and to create a deep learning algorithm.

During the training phase, the model undergoes a process of refining its parameters. This involves an iterative optimization routine, where the model learns from the provided input-output pairs, progressively improving its ability to interpret and analyze data. The validation phase is another critical component of our study. Utilizing 96 samples, this phase is designed to assess the model's performance. It acts as a checkpoint to gauge the effectiveness of the learning that occurred during the training phase. The validation step is instrumental in detecting potential issues like overfitting or underfitting. Finally, 84 testing samples, provide an unbiased evaluation of the model. These samples are distinct from those used in the training and validation phases, ensuring that the test is conducted on data. This approach is important to our methodology as it offers an objective assessment of the model's overall performance.

Figure 2 illustrates the progression of training and validation loss over epochs during a deep learning model's training phase according to mean absolute error. In mathematical terms, Mean Absolute Error (MAE) is defined as:

$$MAE = \frac{1}{n}\sum_{i=1}^{n}|y_i - \widehat{y_i}|$$

3

where n is the number of samples (1024 in our application), y_i is the actual value for the ith sample, $\widehat{y_i}$ is the predicted value for the ith sample. As epochs increase, both losses decrease and tend to converge, showcasing the model's improvement and its ability to generalize from the training data to unseen validation data. In the following, we tested the DCR2D_Net_Archeo algorithm with synthetic and field data.

3. Synthetic Data Applications

According to the second author’s 25 years of experience in archeological prospection, the archeological sites have some common resistivity properties. In general, approximately the first 0.25 to 0.5 meters depth is composed of compressed soil with 60 to 100 Ωm resistivity and underneath this layer, there is soil with %10 to 30% lower resistivity than the surface layer in archeological sites. The buried ancient structures such as stonewalls have 5 to 10 times higher resistivity of the surrounding medium. By using these common features of archeological sites we constructed a 2D resistivity model (Fig. 3). In this

model, there is a 100 Ωm surface layer with 0.5m depth and a basement with 50 Ωm-resistivity. There is a buried 1000-Ωm-resistive body with 2-meter-wide and 1.5-meter-length. This body simulates a buried ancient stonewall cross-section. We randomly changed the resistivity of the first layer, basement, and buried structure. We also randomly changed the size and position of the resistive body and the depth of the surface layer. Finally, we obtained 1080 different resistivity models. During we creation of those models, we consider the depth of penetration according to the current DCR data measurement settings (number of electrodes and electrode spacing and maximum n-level). Those models with their sizes (without resampling) were used to develop the DCR2D_Net_Archeo deep learning algorithm explained in the previous section.

To test the image enhancement of the developed deep learning algorithm, DCR_NET_ARCHAEO, we created five resistivity models that simulate buried archaeological structures such as stonewalls. We calculated the forward response of those models. We added %2 random noise to the data before inversion. In Table 2, the parameters for five distinct resistivity models are given.

The resistivity, and depth of the first, second, and buried resistive rectangular-shaped structures are different in each model. On the other hand, in models 4 and 5, we used two separate buried resistive bodies that can simulate cross-sections of parallel ancient walls. We also considered the depth of penetration of the DCR method during the construction of the test models.

The real resistivity model (first column), the regularized inversion results (second column), and the enhancement of inversion results by using the DCR2D_Net_Archeo algorithm (third column) are illustrated in Fig. 4. As it is expected, regularized inversion gives us a smooth inversion result. We can separate the first layer from the basement. However, resistive body boundaries resolved very smoothly. We also give RMS error for each inversion result in Fig. 4. We used those 2D inversion results in our developed DCR2D_Net_Archeo algorithm. This algorithm improved the image resolution. We also calculated RMS for DCR2D_Net_Archeo algorithm results. The RMS values between the inverted data and calculated data from the enhanced model obtained from the DCR2D_Net_Archeo algorithm are less than 0.01.

The buried resistive structures can clearly be distinguishable if one compares DCR2D_Net_Archeo algorithm results with corresponding real 2D resistivity models. After the enhancement of the 2D resistivity model with the DCR2D_Net_Archeo algorithm, there are some small artifacts seen in the models. The main reason is that we added random noise to the synthetic data and also during the development of the DCR2D_Net_Archeo algorithm we also used random noise-added data inversion results.

Although we just used single resistive structures during the construction of the DCR2D_Net_Archeo algorithm, two separate resistive structures such as in Models 4 and 5 can also be resolved with the developed deep learning algorithm. Synthetic data test showed that the developed DCR2D_Net_Archeo algorithm can enhance 2D DCR data inversion results considerably. In the next section, we test the developed deep learning algorithm in field data.

4. Field Data Applications

We tested our DCR2D_Net_Archeo algorithm with two field data collected in different archeological sites in Türkiye.

4.1. Field Data 1: Roman Bath in Ankara

The first DCR field data was collected in the Roman bath located in Ankara, Türkiye. To examine the defense wall constructed during the latest periods of the Roman Empire and the early years of the Ottoman Empire (Candansayar, 2008). In these archeological sites, DCR data was collected by using a multi-electrode resistivity system with 21 electrodes by using Wenner, Wenner-Schlumberger, dipole-dipole (DD), left- and right-sided pole-dipole (PDL and PDR) arrays. Candansayar (2008) compared the resolution capability of single and combined use of those three- and four-electrode arrays and he suggested that combined use of DD, PDL, and PDR arrays gives a better resolution than individual and combined inversion of the corresponding electrode arrays. According to the DCR inversion result, the location of the buried wall is suggested and after the archaeological excavation, the defense wall was found at 3.5-meter depth (Fig. 5).

In this study we used the DD, PDL, and PDR field data inversion result as input (Fig. 6a) in the developed DCR2D_Net_Archeo algorithm and obtained the 2D enhanced resistivity model (Fig. 6b). We showed the wall anomaly location in the 2D inversion result and enhanced the 2D resistivity model (in Fig. 6) with a white rectangle according to the archaeological excavation in Fig. 5. The developed deep learning algorithm found a clear wall anomaly that exactly fit the excavation result. This result shows that the DCR2D_Net_Archeo algorithm offers more precise spatial and structural information in comparison to traditional DCR data inversion results. These findings suggest that deep learning may offer an approach in archaeogeophysics, providing sharper and more detailed recognition of subsurface remains.

4.2. Field Data 2: Kultepe-Kanesh in Kayseri

The Kültepe-Kanesh archaeological site is located in the Kayseri city, Türkiye. This site was the capital of the ancient Kingdom of Kanesh and the capital city of the earliest international trade system in Anatolia (Kulakoğlu, 2014). The site was first excavated in 1893, modern scientific and interdisciplinary excavations have only been undertaken since 2006 (Atıcı et al. 2014).

The geophysical study was conducted in the area to investigate some stonewall structures built in Asur civilization time. We collected DCR data along 7 parallel lines by using the AGI SuperSting R8/IP data acquisition system in 2018. The data measurement settings are the same as previous field data measurement settings. According to the DCR survey, a 1x4 meter area was suggested for excavation, and a stonewall was found in 2008 (Fig. 7) (Kulakoğlu et al. 2021). The depth of the top part of the wall is approximately 0.6 meters. The 2D inversion result and its enhanced version obtained from the DCR2D_Net_Archeo algorithm are given in Figs. 8a and 8b. Again, it is seen that the buried wall location

can be better resolved with the developed DCR2D_Net_Archeo algorithm if one compares the results with the real excavation result.

5. Conclutions

The most of deep learning-based algorithm developed in recent years, it is suggested to use apparent resistivity data as input and resistivity model as output. The apparent resistivity data set can be very different for the same resistivity model. On the other hand, when one plots the pseudo-section, each PD and DD data is written between potential and current electrodes, on the other hand, W, and WS array data is written between potential electrodes. In this case, if one collects data with a DD array and a deep learning algorithm developed for the Wenner array, the algorithm would fail. On the other hand, the inversion results of different data sets collected by using different arrays along the same line will be very close to each other, and they represent the smooth resistivity model of the underground. Therefore, we suggested using the CNN algorithm to just enhance the resistivity model obtained from the 2D inversion result.

Different from the previous studies, in this study, we suggest using 2D inversion result as input and a real resistivity model for output to develop a U-Net-based CNN algorithm. We developed the DCR2D_Net_Archeo deep learning algorithm to enhance the 2D inversion results of DCR data collected in archaeological sites. In buried archaeological remains, such as stonewalls or ancient graves, resistivity contrast is very high and those structure boundaries are very sharp. The classical regularized smoothing inversion algorithm found some smooth resistivity models and most of these smooth models mask the buried remains location and depth. The developed CNN-based algorithm, DCR2D_Net_Archeo, enhances the 2D inversion result and can recover the archeological remains cross-section. On the other hand, different from the previous deep learning-based algorithm, the developed algorithm does not depend on the electrode arrays used during the data acquisition. We can collect DCR data sets by using various electrode arrays such as WS, DD, PDL, PDR and we can obtain single or combined inversion results of those data sets. The resulting 2D resistivity model can be enhanced by using the DCR2D_Net_Archeooalgorithm.

We showed the success of the developed CNN-based algorithm by using synthetic data. Although the DCR2D_Net_Archeo algorithm is developed by using a 1080 input and output resistivity model that includes just one resistive buried structure, it can recover two buried structures. We also tested the developed algorithm for two different field data collected in two different archaeological sites. We also showed that the DCR2D_Net_Archeo algorithm improves the resistivity image and buried remains depth and location are better recovered than the classical 2D inversion results if one compares with the excavation results.

The developed algorithm can be used for the data collected in any archeological sites if the size of the model is fit. Otherwise, the inversion result can be resampled to get the same size to use the DCR2D_Net_Archeo algorithm. On the other hand, the new deep learning algorithm can be developed for

a specific data set according to the number of electrodes and electrode spacing in a couple of hours by using a Desktop PC.

As a further study, we are planning to develop a CNN-based algorithm to improve 3D DCR data inversion results. The suggested idea can also be applied to other types of 2D/3D geophysical data inversion results such as Magnetotelluric, Seismic, and Ground Penetrating Radar.

Declarations

Author Contribution

The first author developed a Convolutional Neural network-based deep learning algorithm by using the PyTorch library. She also did synthetic data and field data tests with a developed deep learning algorithm. She prepares all the figures. She helps during the writing of the manuscript.The second author modified the DCR2D algorithm to generate a 1080 model. He calculated those model responses and added %2 random noise. Then he inverted synthetic data. He collected field data. He writes the manuscript.

Acknowledgement

This study is part of the first author PhD thesis. This study is also made under the the Ankara University Technopolis R&D projects (STBP code: 084286). We also would like to thank Prof. Fikri Kulakoğlu, head of Kültepe Archaeological Excavation site, for sharing the excavation result in Kültepe. We also thank Cansu Arıcan from Ankara Universiy to help about DCR data format conversion.

References

1. Aghabiglou, A., & Eksioglu, E. M. (2021). Projection-based cascaded U-net model for MR image reconstruction. *Computer Methods and Programs in Biomedicine* 207, 106151. https://doi.org/10.1016/j.cmpb.2021.106151
2. Atici, L., Kulakoglu, F., Fairbairn, A., & Barjamovic, G. (2014). Current Research at Kultepe-Kanesh: An Interdisciplinary and Integrative Approach to Trade Networks, Internationalism, and Identity. Current Research at Kultepe-Kanesh, 1-232.
3. Aleardi, M., Vinciguerra, A. & Azadeh, H. (2021). A convolutional neural network approach to electrical resistivity tomography. *Journal of Applied Geophysics*, 193, 104434. https://doi.org/10.1016/j.jappgeo.2021.104434
4. Aleardi, M., Vinciguerra, A., Stucchi, E. & Hojat, A. (2022). Probabilistic inversions of electrical resistivity tomography data with a machine learning-based forward operator, *Geophysical Prospecting,* 70, 938–957. https://doi.org/10.1111/1365-2478.13189

5. Binley, A., & Kemna, A. (2005). DC resistivity and induced polarization methods. In Hydrogeophysics (pp. 129-156). Dordrecht: Springer Netherlands.
6. Blaschek, R., Hördt, A., & Kemna, A. (2008). A new sensitivity-controlled focusing regularization scheme for the inversion of induced polarization data based on the minimum gradient support. *Geophysics,* 73(2), F45-F54.
7. Candansayar, M.E., (2008). Two-dimensional individual and joint inversion of three- and four-electrode array dc resistivity data. *Journal of Geophysics and Engineering*, 5(3), 290–300. https://doi.org/10.1088/1742-2132/5/3/005
8. Candansayar, M. E., & Tezkan, B. (2008). Two-dimensional joint inversion of radiomagnetotelluric and direct current resistivity data. *Geophysical Prospecting*, 56(5), 737-749. https://doi.org/10.1111/j.1365-2478.2008.00695.x
9. Chambers, J. E., Kuras, O., Meldrum, P. I., Ogilvy, R. D., & Hollands, J. (2006). Electrical resistivity tomography applied to geologic, hydrogeologic, and engineering investigations at a former waste-disposal site. *Geophysics*, 71(6), B231-B239. https://doi.org/10.1190/1.2360184
10. Demirci, İ., Candansayar, M. E., Vafidis, A., & Soupios, P. (2017). Two dimensional joint inversion of direct current resistivity, radio-magnetotelluric and seismic refraction data: An application from Bafra Plain, Turkey. *Journal of Applied Geophysics*, *139*, 316-330. https://doi.org/10.1016/j.jappgeo.2017.03.002
11. Demirci, I., Gündoğdu, N. Y., Candansayar, M. E., Soupios, P., Vafidis, A., & Arslan, H. (2020). Determination and evaluation of saltwater intrusion on bafra plain: joint interpretation of geophysical, hydrogeological and hydrochemical data. *Pure and Applied Geophysics*, 177, 5621-5640. https://doi.org/10.1007/s00024-020-02573-2
12. Feng, J. & Lu, S. (2019). Performance Analysis of Various Activation Functions in Artificial Neural Networks IOP Conf. Series: *Journal of Physics: Conf. Series,* 1237, 022030. https://doi:10.1088/1742-6596/1237/2/022030
13. Gündoğdu, N. Y., Candansayar, M. E. & Genç, E. (2017). Rescue archaeology application: Investigation of Kuriki mound archaeological area (Batman, SE Türkiye) by using direct current resistivity and magnetic methods. *Journal of Environmental and Engineering Geophysics,* 22(2), 177-189. https://doi.org/10.2113/JEEG22.2.177
14. Gündoğdu, N. Y. & Candansayar, M. E. (2018). Three-dimensional regularized inversion of DC resistivity data with different stabilizing functionals. *Geophysics*, 83(6), E399-E407. https://doi.org/10.1190/geo2017-0558.1
15. Gündoğdu, N. Y., Demirci, İ., Demirel, C., & Candansayar, M. E. (2020). Characterization of the bridge pillar foundations using 3d focusing inversion of DC resistivity data. *Journal of Applied Geophysics*, 172, 103875. https://doi.org/10.1016/j.jappgeo.2019.103875
16. Günther, T., Rücker, C. & Spitzer, K. (2006). Three-dimensional modelling and inversion of DC resistivity data incorporating topography—II. Inversion. *Geophysical Journal International,* 166(2), 506-517. https://doi.org/10.1111/j.1365-246X.2006.03011.x

17. Hassan, E., Shams, M. Y., Hikal, N. A. & Elmougy, S. (2022). The effect of choosing optimizer algorithms to improve computer vision tasks: a comparative study. *Multimedia Tools and Applications,* 82, 16591–16633. https://doi.org/10.1007/s11042-022-13820-0
18. Hiskiawan, P., Chen, C. C. & Ye, Z. (2023). Processing of electrical resistivity tomography data using convolutional neural network in ERT-NET architectures, *Arabian Journal of Geosciences,* 16 (581). https://doi.org/10.1007/s12517-023-11690-w
19. Jia, Z., Li, Y., Lu, W., Zhang, L. & Monkam, P. (2022), EMRNet: End-to-End Electrical Model Restoration Network, *IEEE Transactions on Geoscience and Remote Sensing*, 60, 5917912. https://doi.org/10.1109/TGRS.2022.3193297
20. Kulakoğlu, F. (2014). Kanesh after the Assyrian Colony Period: Current research at Kültepe and the Question of the end of the Bronze age settlement. Current Research at Kultepe-Kanesh: An Interdisciplinary and Integrative Approach to Trade Networks, Internationalism, and Identity, 4, 85.
21. Kulakoğlu, F., Kryszat, G. & Michel, C. (2021). Cultural exchanges and current research at Kültepe and its surroundings: Kültepe, 1-4 August, 2019. KIM-Kültepe international meetings,
22. Liu, B., Guo, Q., Li, S., Liu, B., Ren, Y., Pang, Y., Guo, X., Liu, L. & Jiang, P. (2020). Deep Learning Inversion of Electrical Resistivity Data, *IEEE Transactions on Geoscience and Remote Sensing*, 58(8), 5715-5728. https://doi.org/10.1109/TGRS.2020.2969040
23. Liu, B., Guo, Q., Tang, Y. & Jiang, P. (2023). Deep learning inversion method of tunnel resistivity synthetic data based on modelling data, *Near Surface Geophysics*, 21, 249–260. https://doi.org/10.1002/nsg.12253
24. Liu, X., Lu, Q., & Liu, S. (2023). Resolution Enhancement of Electrical Resistivity Tomography Based on Deep Learning, *IEEE Geoscience and Remote Sensing Letters,* 20, 7505505. https://doi.org/10.1109/LGRS.2023.3320698
25. Loke, M. H., Wilkinson, P. B., Chambers, J. E., & Meldrum, P. I. (2018). Rapid inversion of data from 2D resistivity surveys with electrode displacements. *Geophysical Prospecting*, 66(3), 579-594. https://doi.org/10.1111/1365-2478.12522
26. Özyıldırım, Ö., Candansayar, M. E., Demirci, İ., & Tezkan, B. (2017). Two-dimensional inversion of magnetotelluric/radiomagnetotelluric data by using unstructured mesh. *Geophysics*, 82(4), E197-E210. https://doi.org/10.1190/geo2016-0378.1
27. Özyıldırım, Ö., Demirci, İ., Gündoğdu, N. Y., & Candansayar, M. E. (2020). Two dimensional joint inversion of direct current resistivity and radiomagnetotelluric data based on unstructured mesh. *Journal of Applied Geophysics*, 172, 103885. https://doi.org/10.1016/j.jappgeo.2019.10388
28. Parasnis, D. (2013). *Mining geophysics* (Vol. 3). Elsevier.
29. Ronneberger, O., Fischer, P., & Brox, T. (2015). U-Net: Convolutional Networks for Biomedical Image Segmentation. In International Conference on Medical image computing and computer-assisted intervention, (volume 9351, pp. 234-241). Lecture Notes in Computer Science.
30. Sasaki, Y. (1994). 3-D resistivity inversion using the finite-element method. *Geophysics*, 59(12), 1839-1848. https://doi.org/10.1190/1.1443571

31. Sasaki, Y. (1989). Two-dimensional joint inversion of magnetotelluric and dipole-dipole resistivity data. *Geophysics*, *54*(2), 254-262. https://doi.org/10.1190/1.1442649
32. Soupios, P. M., Kouli, M., Vallianatos, F., Vafidis, A., & Stavroulakis, G. (2007). Estimation of aquifer hydraulic parameters from surficial geophysical methods: A case study of Keritis Basin in Chania (Crete–Greece). *Journal of Hydrology*, 338(1-2), 122-131. https://doi.org/10.1016/j.jhydrol.2007.02.02
33. Thibaut, R., Kremer, T., Royen, A., Ngun, B. K., Nguyen, F., & Hermans, T. (2021). A new workflow to incorporate prior information in minimum gradient support (MGS) inversion of electrical resistivity and induced polarization data. *Journal of Applied Geophysics*, 187, 104286. https://doi.org/10.1016/j.jappgeo.2021.104286
34. Wisén, R., Christiansen, A. V., Dahlin, T., & Auken, E. (2008). Experience from two resistivity inversion techniques applied in three cases of geotechnical site investigation. *Journal of geotechnical and geoenvironmental engineering*, *134*(12), 1730-1742. https://doi.org/10.1061/(ASCE)1090-0241(2008)134:12(1730)

Tables

Table 1 and 2 are available in the Supplementary Files section.

Figures

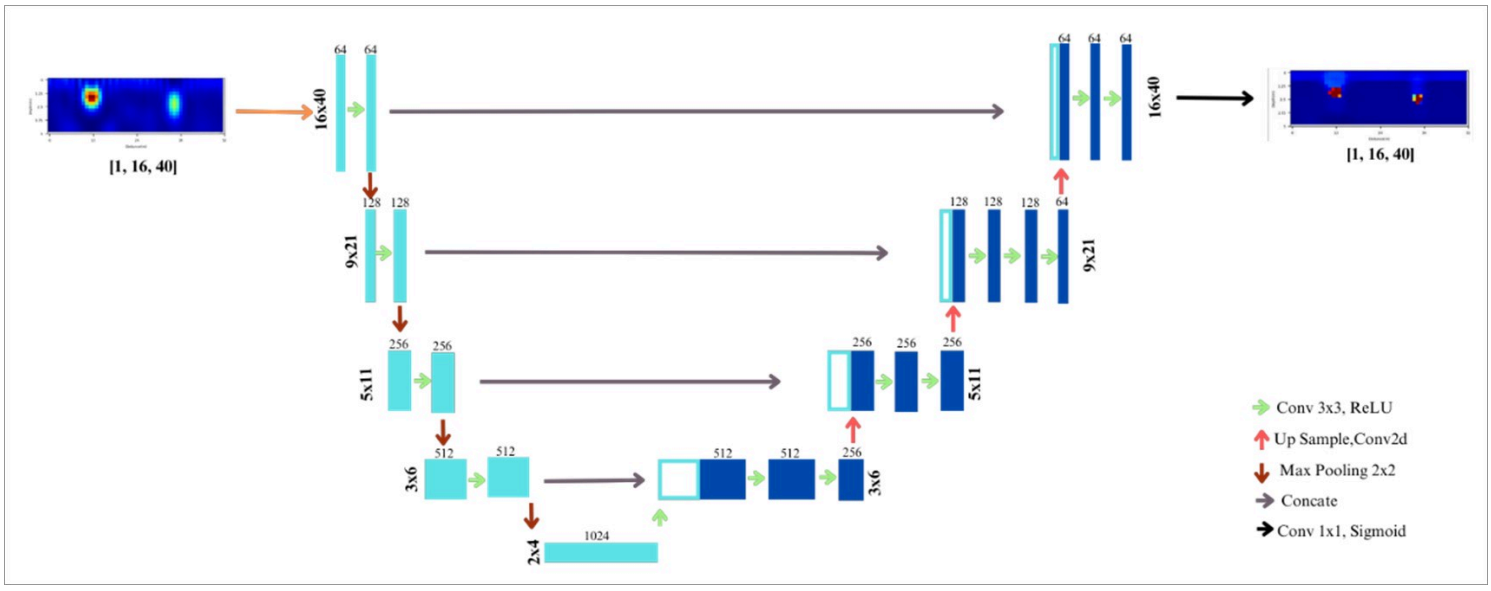


Figure 1

The used U-Net architecture in this study. This architecture features a comprehensive four-layer encoder-decoder structure, totaling 23 layers. The network takes traditional inversion results as input data and real models as output data.

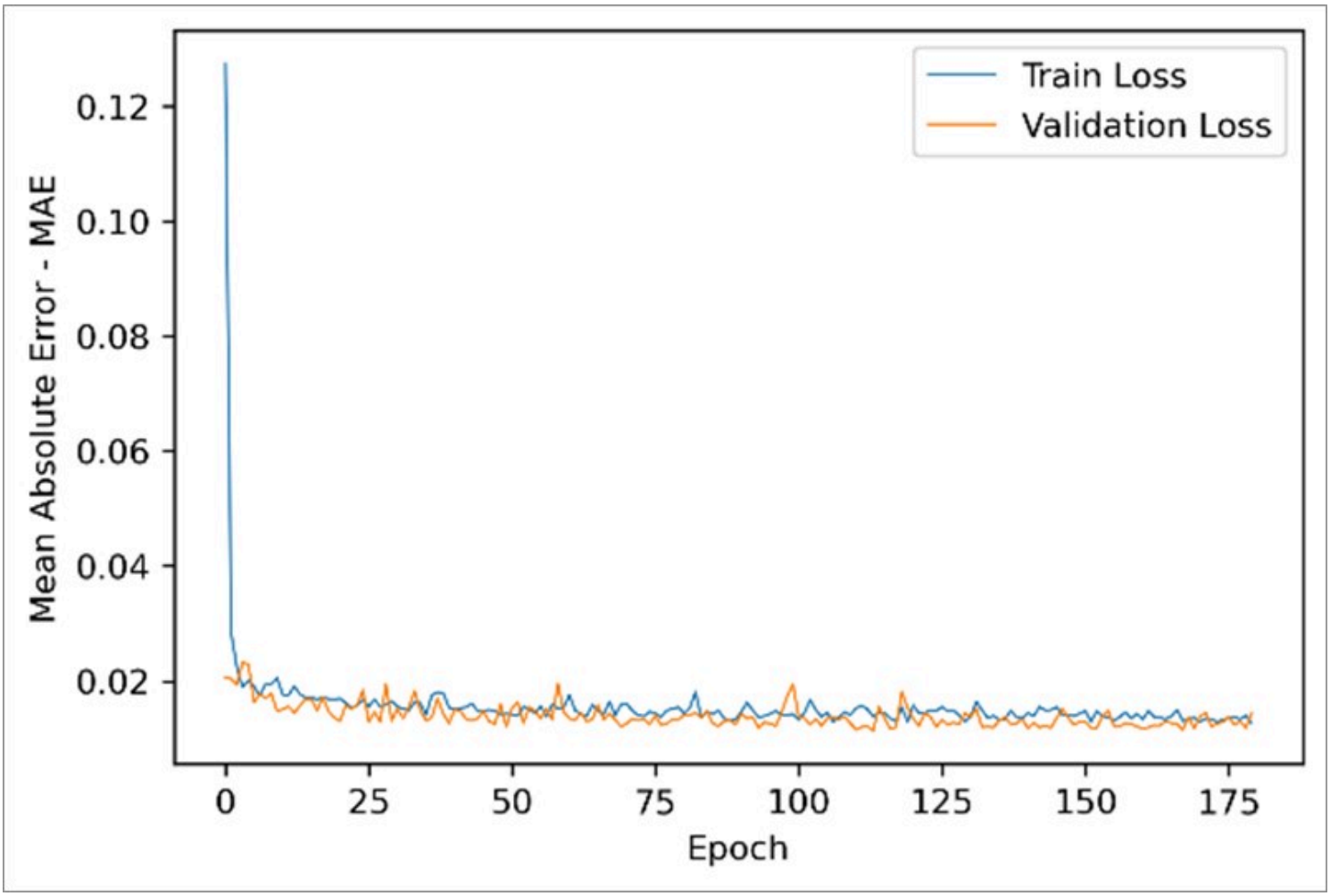


Figure 2

Mean absolute error of training and validation loss in each epoch during DCR2D_Net_Archeo algorithm development.

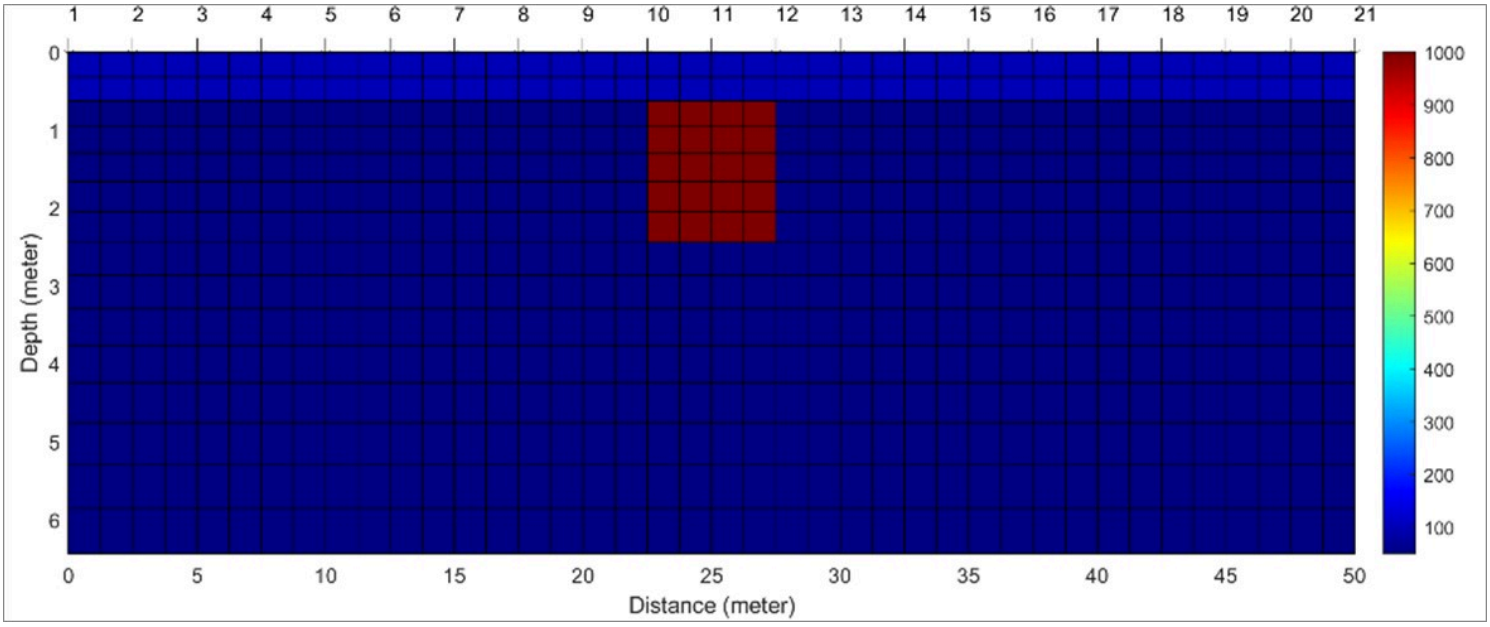


Figure 3

The base 2D resistivity model simulates classical archeological sites in Türkiye. The 1080 resistivity model was obtained from a variation of this model.

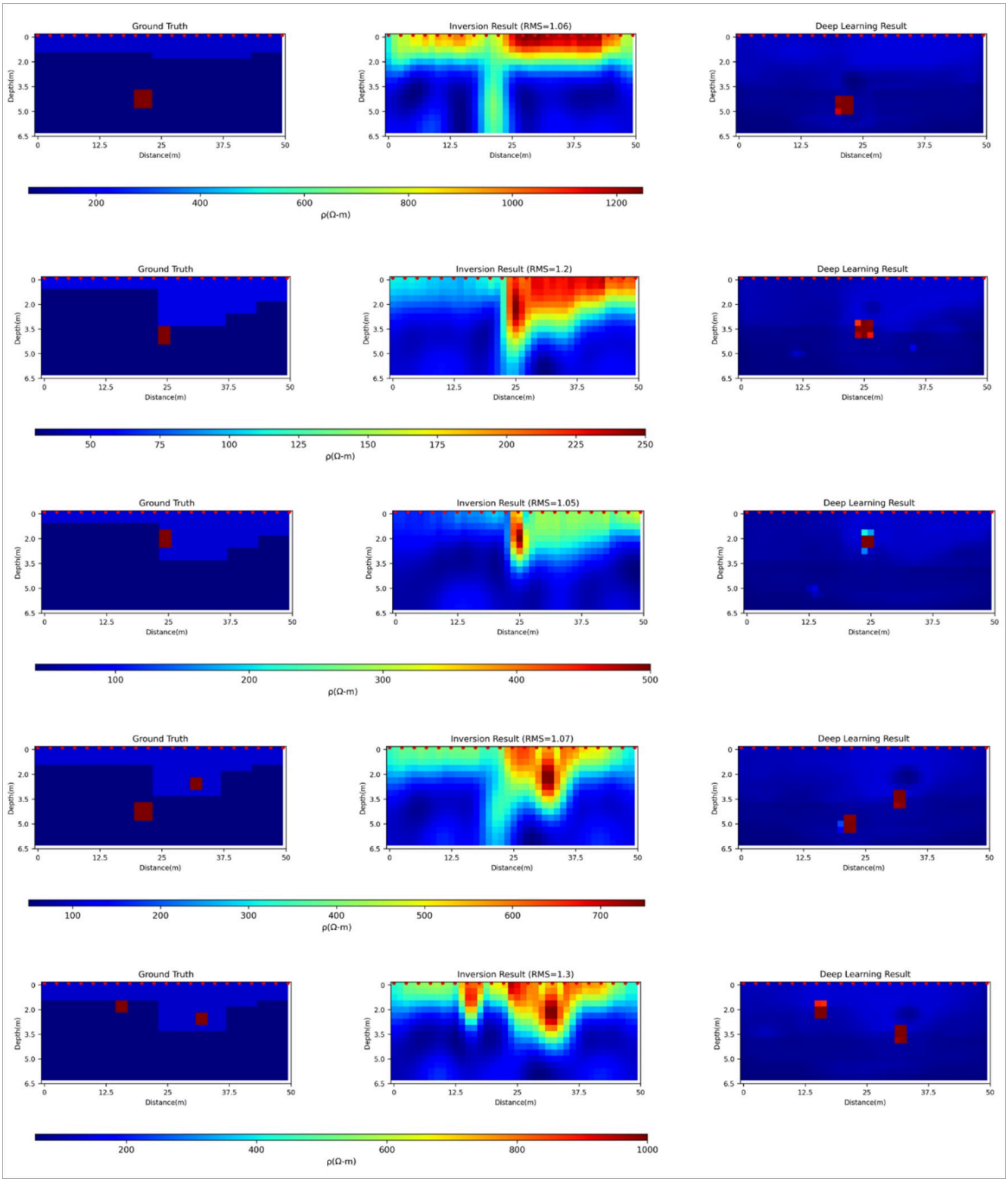


Figure 4

Comparison of 2D resistivity models: Real Models (first column), 2D inversion results (second column) of synthetic data obtained from the real models given in the first column, and DCR2D_Net_Archeo results (third column).

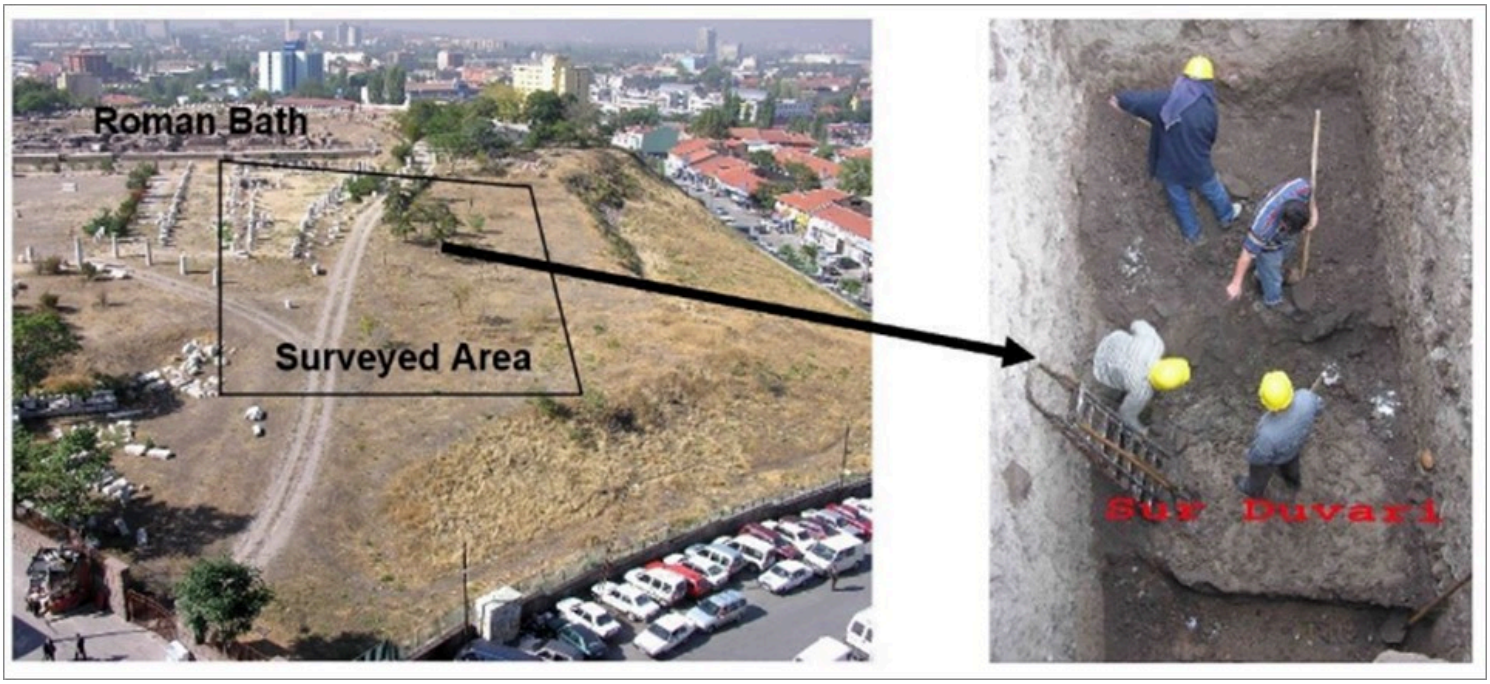


Figure 5

The ancient Roman bath at Ankara, Türkiye, and excavated wall photo in the area (taken from Candansayar 2008)

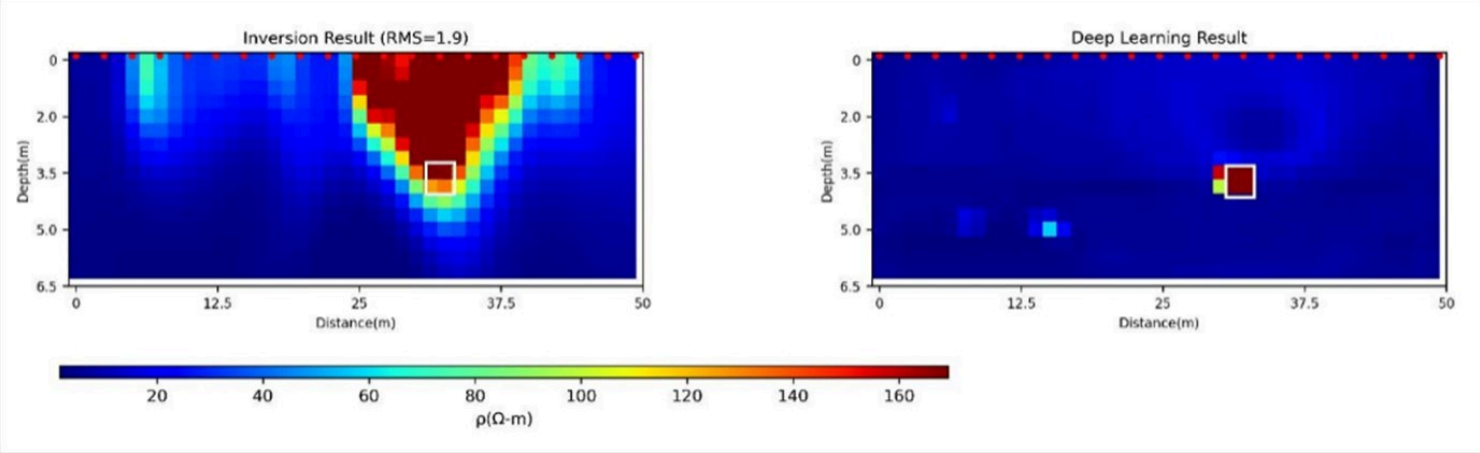


Figure 6

(a) Field data, collected from the Roman Bath archaeological site, 2D inversion result, and (b) Enhancement of the resistivity model by using DCR2D_Net_Archeo. The white rectangle shows the excavated Roman time defense wall location.



Figure 7

Aerial photo of the excavated wall according to DCR survey in 2008 (photo taken by Kulakoğlu et al. 2021)

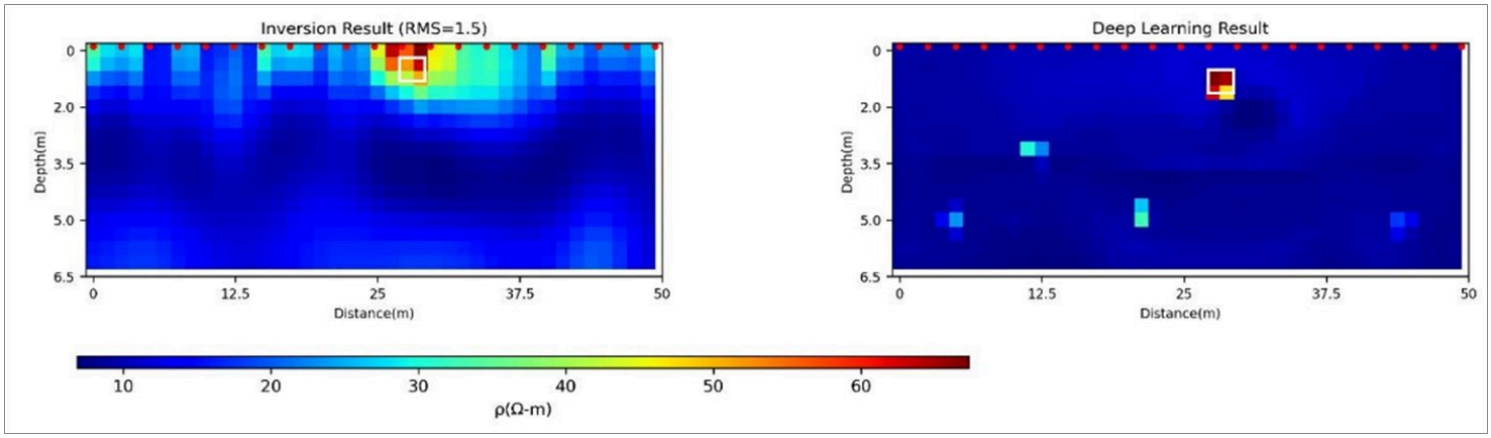


Figure 8

(a) Field data, collected from the Kultepe archaeological site, 2D inversion result, and (b) Enhancement of the resistivity model by using DCR2D_Net_Archeo. The white rectangle shows the excavated ancient wall location.

Supplementary Files

This is a list of supplementary files associated with this preprint. Click to download.

- 3Tables.docx